Research Article

Sajid Hussain, Asim Aziz*, Chaudhry Masood Khalique, and Taha Aziz

Numerical investigation of magnetohydrodynamic slip flow of power-law nanofluid with temperature dependent viscosity and thermal conductivity over a permeable surface

https://doi.org/10.1515/phys-2017-0104
Received Aug 03, 2017; accepted Oct 16, 2017

Abstract: In this paper, a numerical investigation is carried out to study the effect of temperature dependent viscosity and thermal conductivity on heat transfer and slip flow of electrically conducting non-Newtonian nanofluids. The power-law model is considered for water based nanofluids and a magnetic field is applied in the transverse direction to the flow. The governing partial differential equations(PDEs) along with the slip boundary conditions are transformed into ordinary differential equations(ODEs) using a similarity technique. The resulting ODEs are numerically solved by using fourth order Runge-Kutta and shooting methods. Numerical computations for the velocity and temperature profiles, the skin friction coefficient and the Nusselt number are presented in the form of graphs and tables. The velocity gradient at the boundary is highest for pseudoplastic fluids followed by Newtonian and then dilatant fluids. Increasing the viscosity of the nanofluid and the volume of nanoparticles reduces the rate of heat transfer and enhances the thickness of the momentum boundary layer. The increase in strength of the applied transverse magnetic field and suction velocity increases fluid motion and decreases the temperature distribution within the boundary layer. Increase in the slip velocity enhances the rate of heat transfer whereas thermal slip reduces the rate of heat transfer.

Keywords: Non-Newtonian nanofluids; Power-law model; Brickman nanofluid Model; Temperature dependent viscosity; Temperature dependent thermal conductivity; Partial slip; Magnetohydrodynamics

PACS: 44.20.+b, 44.40.+a, 47.10.-g, 47.15.-x

1 Introduction

In recent years, gradual development in fluid dynamics has resulted active studies of nanofluids, due to their applications in different industrial sectors. Choi [1] first introduced the term nanofluids and demonstrated theoretically the validity of the concept by including nano-sized particles in ordinary fluids. Eastman *et al.* [2] observed an unusual thermal conductivity enhancement in copper-water nanofluids at small nanoparticle volume fraction. Experiments performed by [3–5] confirm that the thermal conductivity of nanofluids is higher than the thermal conductivity of ordinary fluids. Buongiorno [6] theoretically observed that the properties of nanofluids like wetting, spreading and dispersion on a solid surface are better and more stable when compared to ordinary fluids. A comprehensive literature survey on slip flow of nanofluids under different thermo-physical situations is presented in[7–18]. In addition to the above studies Vahabzadeh *et al.* [19] obtained the analytical solutions of nanofluid flow over a horizontal stretching surface with variable magnetic field and viscous dissipation effects. They employed the homotopy perturbation method, Adomian decomposition method, and variational iteration method to determine the solution for the nanofluid flow and heat transfer characteristics within the boundary layer. Comparisons

***Corresponding Author: Asim Aziz:** College of Electrical and Mechanical Engineering, National University of Sciences and Technology, 45000, Rawalpindi, Pakistan; Email: aaziz@ceme.nust.edu.pk

Sajid Hussain: Department of Mathematics, Capital University of Science and Technology, Islamabad, Pakistan; Email: prsajid@yahoo.com

Chaudhry Masood Khalique: International Institute for Symmetry Analysis and Mathematical Modeling, Department of Mathematical Sciences, North-West University, Mafikeng Campus, Private Bag X2046, Mmabatho 2735, South Africa; Email: Masood.Khalique@nwu.ac.za

Taha Aziz: School of Computer, Statistical and Mathematical Sciences, North-West University, Potchefstroom Campus, Private Bag X6001, Potchefstroom 2531, South Africa; Email: tahaaziz77@yahoo.com

are also drawn with solutions obtained through numerical techniques. Similar to Vahabzadeh, Anwar *et al.* [20] used the variation iteration method to study the flow of nanofluid over an exponentially stretching surface within a porous medium.

The aforementioned studies and comprehensive literature review on convective transport of nanofluids reveal that non-Newtonian models for nanofluids have not received much attention. Some authors considered non-Newtonian models for the study of nanofluids, for example, Santra *et al.* [21] numerically studied forced convective flow of *Cu*-water nanofluid in a horizontal channel. They considered the power-law model for a non-Newtonian nanofluid and concluded that the rate of heat transfer increases due to increase in the volume of nanoparticles. Ellahi *et al.* [22] presented series solutions for flow of third-grade nanofluids considering both the Reynolds and Vogels model. Flow and heat transfer analysis of Maxwell nanofluids over a stretching surface was considered by Nadeem *et al.* [23]. Ramzan and Bilal [24] studied unsteady MHD second grade incompressible nanofluid flow towards a stretching sheet. Hayat *et al.* [25] examined the influence of convective boundary conditions on power-law nanofluid. Khan and Khan [26] presented a numerical investigation on MHD flow of power-law nanofluid induced by nonlinear stretching of a flat surface. Moreover, Aziz *et al.*[27] found exact solutions for the Stokes' flow of a non-Newtonian third grade nanofluid model using a Lie symmetry approach. In addition to the above, the models for non-Newtonian nanofluid are well discussed in [28–30].

To the best of the authors' knowledge no research has been conducted to study MHD slip flow of power-law nanofluids having variable thermo-physical properties over a permeable flat surface. In the present research, we investigate slip flow of an electrically conducting power-law nanofluid over a permeable flat surface with power-law wall slip condition and temperature dependent viscosity and thermal conductivity. The forth order RK method with shooting technique is employed to obtain solutions numerically. The influence of various physical parameters on the behavior of velocity and temperature of *Cu*-water nanofluid, with skin friction coefficient and the Nusselt number is discussed in detail.

2 Physical model and formulation

Consider the steady, laminar flow of an incompressible electrically conducting non-Newtonian nanofluid over a permeable flat surface. The power-law non-Newtonian fluid model is assumed for the water based nanofluid and power-law velocity slip condition is employed at the boundary. A uniform magnetic field is applied in the transverse direction to the flow. The viscosity and the thermal conductivity vary with temperature T. The porosity of the surface is considered as uniform and the uniform magnetic field of strength B_o is applied in the direction perpendicular to sheet. The induced magnetic field is considered negligible when compared to the applied magnetic field. In view of the above assumptions, as well as of the usual boundary layer approximations the governing equations are thus:

$$\frac{\partial u}{\partial x} + \frac{\partial v}{\partial y} = 0, \tag{1}$$

$$u\frac{\partial u}{\partial x} + v\frac{\partial u}{\partial y} = \frac{1}{\rho_{nf}}\frac{\partial}{\partial y}\left[\mu_{nf}(T)\left|\frac{\partial u}{\partial y}\right|^{n-1}\frac{\partial u}{\partial y}\right] - \frac{\sigma_{nf}}{\rho_{nf}}B_0^2(u - U_\infty), \tag{2}$$

and

$$u\frac{\partial T}{\partial x} + v\frac{\partial T}{\partial y} = \frac{1}{(\rho C_p)_{nf}}\frac{\partial}{\partial y}\left[\kappa_{nf}(T)\frac{\partial T}{\partial y}\right]. \tag{3}$$

Here u is a component of velocity along the direction of the flow and v is the velocity perpendicular to it. $\mu_{nf}(T)$, ρ_{nf}, σ_{nf}, $(C_p)_{nf}$, $\kappa_{nf}(T)$ refer to nanofluid dynamic viscosity, density, electrical conductivity, specific heat capacity of nanofluid at fixed pressure and thermal conductivity respectively. Moreover, U_∞ is the velocity far away from the surface known as the free stream velocity and n is the power-law index.

The appropriate conditions for the modeled problem are:

$$u(0) = L_1\left(\frac{\partial u}{\partial y}\right)^n, \quad v(0) = V_w, \quad u_{y\to\infty} = U_\infty \tag{4}$$

$$T(0) = T_w + D_1\frac{\partial T}{\partial y}, \quad T_{y\to\infty} = T_\infty, \tag{5}$$

where T_w is the surface temperature and T_∞ is the temperature outside the boundary layer, $L_1 = L_0\sqrt{R_{e_x}}$ and $D_1 = D_0\sqrt{R_{e_x}}$ are the velocity and thermal slip factors with L_0 as initial velocity slip, D_0 as initial thermal slip and $R_{e_x} = \frac{\rho_f x^n}{\mu_f U_\infty^{(n-2)}}$ is the local Reynolds number. Finally, V_w is the constant suction/injection velocity across the surface. Commonly used property relations for nanofluids are presented as (for details see [31–33]):

$$\mu_{nf}(T) = \mu_{nf}^\star\left[a + b(T_w - T)\right], \tag{6}$$
$$\kappa_{nf}(T) = \kappa_{nf}^\star\left[1 + \epsilon\frac{T - T_\infty}{T_w - T_\infty}\right],$$

$$\rho_{n_f} = (1-\phi)\rho_f + \phi\rho_s, \tag{7}$$
$$(\rho C_p)_{n_f} = (1-\phi)(\rho C_p)_f + \phi(\rho C_p)_s,$$

$$\mu^{\star}_{n_f} = \frac{\mu_f}{(1-\phi)^{2.5}}, \tag{8}$$
$$\frac{\kappa^{\star}_{n_f}}{\kappa_f} = \frac{(\kappa_s + 2\kappa_f) - 2\phi(\kappa_f - \kappa_s)}{(\kappa_s + 2\kappa_f) + \phi(\kappa_f - \kappa_s)},$$

and

$$\frac{\sigma_{n_f}}{\sigma_f} = \left[1 + \frac{3(\frac{\sigma_s}{\sigma_f} - 1)\phi}{(\frac{\sigma_s}{\sigma_f} - 2) - (\frac{\sigma_s}{\sigma_f} - 1)\phi}\right]. \tag{9}$$

In Eqs. (6)-(9), $\mu^{\star}_{nf}$ is the effective dynamic viscosity of the nanofluid, $\kappa^{\star}_{nf}$ is a constant thermal conductivity with ϵ as a parameter, a and b are positive constants, ϕ is the volume fraction of solid nanoparticles in the base fluid, ρ_f, $(Cp)_f$, μ_f, κ_f and σ_f are the density, specific heat capacity, coefficient of viscosity, thermal conductivity and the electrical conductivity of the base fluid. Whereas ρ_s, $(Cp)_s$, μ_s, κ_s and σ_s are the density, specific heat capacity, coefficient of viscosity, thermal conductivity and electrical conductivity of the nanoparticles respectively.

In order to solve the governing boundary value problem (1)-(3), the stream function $\psi(x, y)$ is introduced which identically satisfies Eq. (1) with

$$u = \frac{\partial\psi}{\partial y} \quad \text{and} \quad v = -\frac{\partial\psi}{\partial x}. \tag{10}$$

Equations (2)-(3) after utilizing Eqs. (6)-(10), are transformed into

$$\frac{\partial\psi}{\partial y}\frac{\partial^2\psi}{\partial x\partial y} - \frac{\partial\psi}{\partial x}\frac{\partial^2\psi}{\partial y^2} = \frac{\mu^{\star}_{nf}}{\rho_{nf}}\left[-b\frac{\partial T}{\partial y}\left|\frac{\partial^2\psi}{\partial y^2}\right|^{n-1}\frac{\partial^2\psi}{\partial y^2}\right] \tag{11}$$
$$-\frac{\sigma_{nf}}{\rho_{nf}}B^2\left(\frac{\partial\psi}{\partial y} - u_\infty\right) + \frac{\mu^{\star}_{nf}}{\rho_{nf}}\left[\left[a + b(T_w - T)\right]\left\{(n-1)\left|\frac{\partial^2\psi}{\partial y^2}\right|^{n-1}\left(\frac{\partial^2\psi}{\partial y^2}\right)^2\frac{\partial^3\psi}{\partial y^3} + \left|\frac{\partial^2\psi}{\partial y^2}\right|^{n-1}\frac{\partial^3\psi}{\partial y^3}\right\}\right]$$

and

$$\frac{\partial\psi}{\partial y}\frac{\partial T}{\partial x} - \frac{\partial\psi}{\partial x}\frac{\partial T}{\partial y} = \frac{\kappa^{\star}_{nf}}{(\rho C_p)_{nf}}\left[\frac{\epsilon}{T_w - T_\infty}\right]\left(\frac{\partial T}{\partial y}\right)^2 \tag{12}$$
$$+ \frac{\kappa^{\star}_{nf}}{(\rho C_p)_{nf}}\left[1 + \epsilon\frac{T - T_\infty}{T_w - T_\infty}\right]\frac{\partial^2 T}{\partial y^2}.$$

Boundary conditions (4) are likewise transformed into

$$\frac{\partial\psi}{\partial y} = L_1\left(\frac{\partial^2\psi}{\partial y^2}\right)^n, \quad \frac{\partial\psi}{\partial x} = -V_w, \tag{13}$$
$$\text{at} \quad y = 0; \quad \frac{\partial\psi}{\partial y} \to 0 \quad \text{as} \quad y \to \infty.$$

The following dimensionless similarity variable and similarity transformations are introduced into Eqs. (11)-(12)

$$\eta = \left(\frac{R_e}{x/L}\right)^{\frac{1}{n+1}}\frac{y}{L}, \tag{14}$$
$$\psi(x, y) = LU_\infty\left(\frac{x/L}{R_e}\right)^{\frac{1}{n+1}}f(\eta), \quad \theta(\eta) = \frac{T - T_\infty}{T_w - T_\infty},$$

where θ is the dimensionless temperature and $R_e = \frac{\rho_f L^n}{\mu_f U_\infty^{(n-2)}}$ is the generalized Reynolds number.

The system (11)-(12) is reduced into a self-similar system of ordinary differential equations

$$n(a + A - A\theta)|f''|^{n-1}f''' + (\phi_2/\phi_1)\left(\frac{1}{n+1}\right)ff'' \tag{15}$$
$$- A\theta'|f''|^n - (\phi_4/\phi_1)M(f' - 1) = 0,$$

$$(1 + \epsilon\theta)\theta'' + \frac{1}{n+1}(\phi_3/\phi_5)P_r f\theta' + \epsilon\theta'^2 = 0. \tag{16}$$

Here $M = \frac{\sigma_f B^2 x}{\rho_f U_\infty}$ is the magnetic parameter, $A = b(T_w - T_\infty)$ is the viscosity parameter,
$P_{rx} = \frac{(\rho C_p)_f L^2 U_\infty}{\kappa_f x}$ is the local Prandtl number and

$$\phi_1 = (1-\phi)^{2.5}, \quad \phi_2 = \left((1-\phi) + \phi\frac{\rho_s}{\rho_f}\right),$$
$$\phi_3 = \left((1-\phi) + \phi\frac{(\rho C_p)_s}{(\rho C_p)_f}\right),$$
$$\phi_4 = \left(1 + \frac{3(r-1)\phi}{(r-2) - (r-1)\phi}\right),$$
$$\phi_5 = \left(\frac{(k_s + 2k_f) - 2\phi(k_f - k_s)}{(k_s + 2k_f) + \phi(k_f - k_s)}\right), \quad r = \frac{\sigma_s}{\sigma_f}.$$

Similarly, the boundary conditions in equation(13) are transformed to

$$f(0) = S, \quad f'(0) = 1 + \delta(f''(0))^n, \tag{17}$$
$$\theta(0) = 1 + \gamma\theta'(0),$$

$$f'(\eta) \to 1, \quad \theta(\eta) \to 0, \quad \text{as} \quad \eta \to \infty, \tag{18}$$

where $S = -\frac{(n+1)x^{\frac{n}{n+1}}}{(U_\infty)^{\frac{2n-1}{n+1}}}\left(\frac{\rho_f}{\mu_f}\right)^{\frac{1}{n+1}}V_w$ is the suction/injection parameter, $\delta = \frac{L^{\frac{n+2}{2}}}{(U_\infty)^{\frac{n(n-5)}{2n+2}}}\left(\frac{\rho_f}{\mu_f}\right)^{\frac{3n+1}{2n+2}}$ is the velocity slip parameter and $\gamma = D\left(\frac{L^{n(n+2)}}{x}\right)^{\frac{1}{n+1}}\left(\frac{\rho_f}{\mu_f}\right)^{\frac{n+3}{n+1}}$ is the thermal slip parameter.

3 Numerical solution

The governing equation (15)-(16) with their associated boundary conditions (17)-(18) are solved numerically using the fourth order Runge-Kutta method with a shooting

Table 1: Values of skin friction = $-f''(0)$ and Nusselt number = $-\theta'(0)$ for natural convective MHD flow of power-law nanofluid with slip at the boundary

n	M	P_r	δ	γ	$-f''(0)$[34]	$-\theta'(0)$[34]	Present $-f''(0)$	Present $-\theta'(0)$
0.4	0.6	0.7	0.3	0.3	0.82269	0.39319	0.822690	0.393190
1.0					0.68047	0.33497	0.680471	0.334972
1.4					0.67638	0.31484	0.676380	0.314843
1.4	0.6	0.7	0.3	0.0	0.50701	0.34768	0.50701	0.347683
1.4	0.6	0.7	0.3	0.6	0.67638	0.28767	0.676380	0.287672
1.4	1.0	0.7	0.3	0.3	0.78586	0.32410	0.785860	0.324101

method. For the present, flow and heat transfer analysis, system (15)-(16) is first reduced to

$$f' = g, \quad g' = h,$$
$$h' = \frac{1}{n(a+A-A\theta)|h|^{n-1}}\left[-\left(\frac{1}{n+1}\right)(\phi_2/\phi_1)fh + Az|h|^n + (\phi_4/\phi_1)M(g-1)\right],$$

$$\theta' = p, \quad p' = \frac{1}{1+\epsilon\theta}\left[-\frac{1}{n+1}(\phi_3/\phi_5)P_r fp - \epsilon p^2\right]$$

where $n \neq 1$,

$$f(0) = S, \quad g(0) = \delta(h(0))^n, \quad \theta(0) = 1 + \gamma p(0),$$
$$h(0) = G_1, \quad p(0) = G_2,$$

where G_1 and G_2 are missing values which are chosen by a hit and trial method (as guesses) such that the boundary conditions $g(\infty)$ and $\theta(\infty)$ are satisfied.

Numerical computations are performed taking a uniform step size $\Delta\eta = 0.01$ so that smoothness in the convergent solutions is obtained with an error of tolerance 10^{-6}. Errors are inevitable due to the unbounded domain, whereas the computational domain must be finite. The step size and the position of the edge of the boundary layer are adjusted for different values of the governing parameters to maintain convergence of the numerical solution. Details of the solution procedure are not presented here for brevity. To confirm the numerical procedure, using the proposed code, the present results are compared with results available in the literature. The test case is natural convection of MHD boundary layer flow of power-law nanofluid over a surface (flat) having power-law slip. Comparison of our results and results of other investigators is shown in Table 1. These results are obtained for $a = 1$, $\phi = A = \epsilon = S = 0$. As can be seen from Table 1, the present results and the results presented by Hirschhorn *at el.* [34] show excellent agreement, for both the Nusselt number and the skin friction coefficient.

4 Results and discussion

A numerical investigation has been carried out to study flow of fluid and variations in temperature of a Cu-water power-law nanofluid within a boundary layer. To demonstrate the meaningful relationship between the parameters, *i.e*, n, A, ϵ, ϕ, M, S, δ and γ, numerically obtained results are presented in the form of graphs for variations in velocity $f'(\eta)$ and temperature $\theta(\eta)$ profiles. The behavior of frictional drag and heat transfer rate at the flat surface are also calculated with variation in the governing parameters and tabulated in Table 1. Material properties of Cu-water nanofluid are tabulated in Table 2 (see for example, B. Shankar and Y. Yirga [35]). Graphs of our results are drawn for fixed values of $Pr = 6.2$ and $a = 1.0$, while varying parameters A, M, ϕ, ϵ, S, δ and γ.

Table 2: Properties of Copper-Water Nanofluid

Material Properties	Units	Water	$Cu(300 - Kelvin)$
Density ρ	(kg/m^3)	997.1	8933
Specific heat Cp	(J/kgK)	4179	385
Thermal conductivity κ	(W/mK)	0.613	401
Electrical conductivity σ	$(\Omega.m)^{-1}$	0.05	5.96×10^7

The effect of temperature dependent viscosity on velocity of Newtonian ($n = 1$), pseudoplastic ($n < 1$) and dilatant ($n > 1$) fluids is presented in Figure 1. We have chosen an arbitrary value $n = 0.4$ for pseudoplastic and $n = 1.4$ for dilatant nanofluids. The curves in Figures 1 follow the general trend, *i.e*, fluid motion within the boundary layer will decrease due to an increase in resistance in the fluid caused by increasing the viscosity parameter. Moreover, for a fixed value of the viscosity parameter (say, $A = 0.6$), the effect of the power-law index n on the velocity

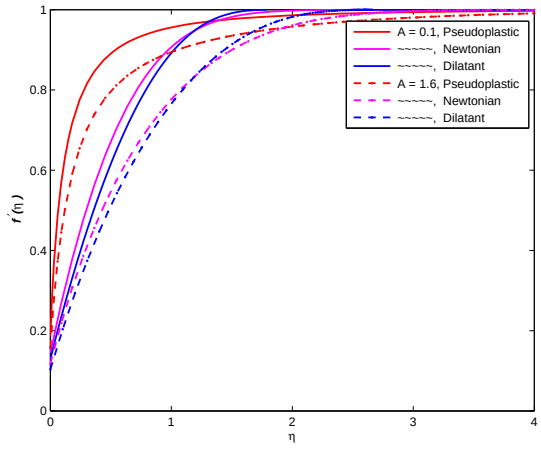

Figure 1: Influence of A on velocity of a power-law nanofluid when $a = 1, M = 0.2, \phi = 0.2, \epsilon = 0.3, Pr = 6.2, S = 0.4, \delta = 0.1, \gamma = 0.6$

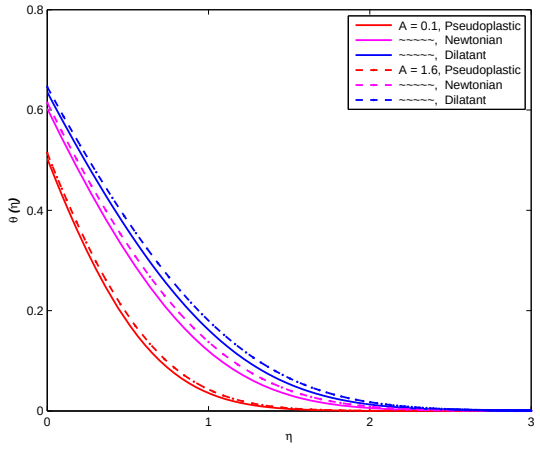

Figure 2: Influence of A on temperature of a power-law nanofluid when $a = 1, M = 0.2, \phi = 0.2, \epsilon = 0.3, Pr = 6.2, S = 0.4, \delta = 0.1, \gamma = 0.6$

profiles of non-Newtonian nanofluids can be observed in Figure 1. Initially fluids with pseudoplastic behavior move fastest within the boundary layer, whereas the velocity of dilatant fluids is the slowest. The reason behind this is the lowest effective viscosity of pseudoplastic fluids. This trend is reversed in the range where shear stress becomes more dominant and the viscosity of pseudoplastic fluids becomes highest. The temperature distribution of a power-law nanofluid effected by variation in the fluid viscosity is shown in Figure 2. The effect of increasing the value of A, leads to thickening of the thermal boundary layer, which results in an increase in temperature and a decrease in heat transfer. This behavior is very noticeable in shear thickening fluids when compared to Newtonian and shear thinning fluids.

Figures 3 and 4 depict the velocity and temperature profiles of power-law non-Newtonian nanofluid for variation in ϵ when $M = \phi = A = 0.2, S = 0.4, \delta = 0.1, \gamma = 0.6$. It is clear from Figure 3, that the thermal conductivity parameter has no effect on the velocity profiles of nanofluid. However, increasing values of the index n, show thickening of the momentum boundary layer in some initial range of η and subsequently thinning of the momentum boundary layer thickness is observed. The reason for this behavior has already been explained in the preceding discussion of Figure 1. Analysis of curves in Figure 4 illustrates that nanofluid temperature rises within the boundary layer with a rise in thermal conductivity and tends asymptotically to zero as the distance from the boundary increases. This fact is clear from our definition, $\kappa_{nf} > \kappa^{\star}_{nf}$ for $\epsilon > 0$, $i.e.$, the thermal conductivity of a nanofluid increases with increasing values of ϵ.

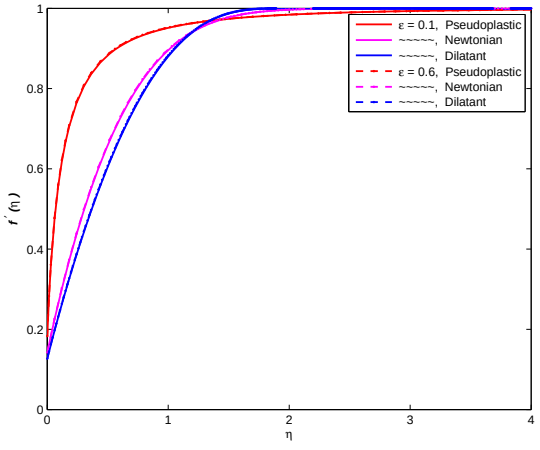

Figure 3: Influence of ϵ on velocity of a power-law nanofluid

The variation in M (strength of applied transverse magnetic field) and its effect on nanofluid velocity is presented in Figure 5 for parameter values $A = \phi = 0.2, \epsilon = 0.3, S = 0.4, \delta = 0.1, \gamma = 0.6$. The curves with index $n = 1.4$, indicate that thickness of the momentum boundary layer decreases with increasing value of M. In other words, the increasing strength of the magnetic parameter M boosts flow of the nanofluid within the boundary layer. In this case, the Lorentz force (generated due to application of a transverse magnetic field) counteracts the viscous forces and enhances nanofluids motion. Figure 6 presents variation in temperature profiles under slip conditions for different values of M. As the parameter M increases the temperature of the power-law nanofluid decreases within the boundary layer. This is because increasing the value

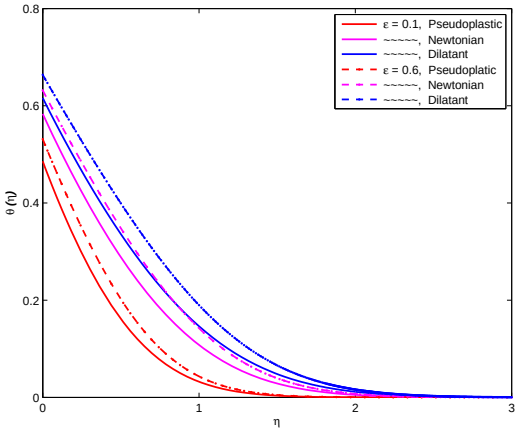

Figure 4: Influence of ϵ on the temperature of a power-law nanofluid

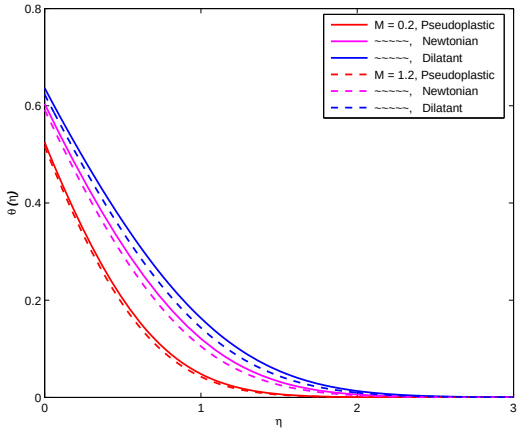

Figure 6: Influence of M on temperature of a power-law nanofluid

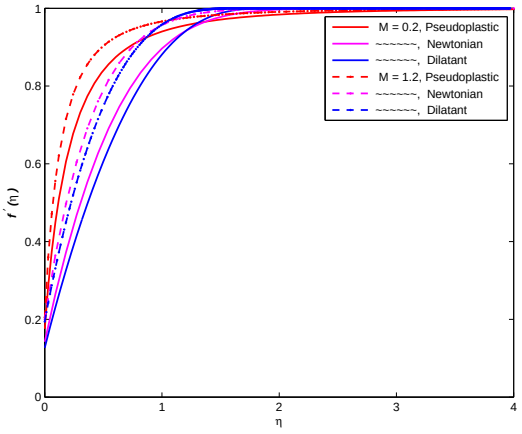

Figure 5: Influence of M on velocity of a power-law nanofluid

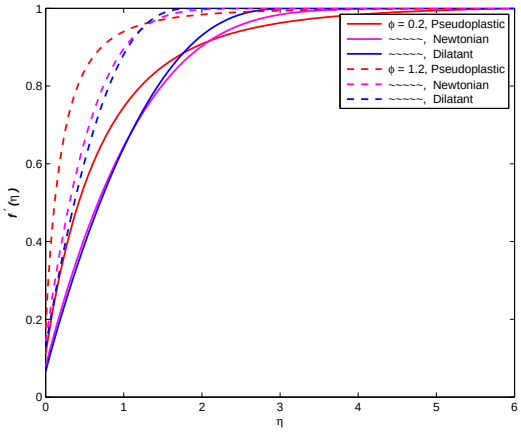

Figure 7: Influence of ϕ on velocity of a power-law nanofluid

of the strength of the transverse magnetic field boosts the fluid velocity within the boundary layer.

Figures 7 and 8 display that both the nanofluid velocity and temperature within the boundary layer increase with increasing values of ϕ when $A = M = 0.2$, $\epsilon = 0.3$,$S = 0.4$, $\delta = 0.1$, $\gamma = 0.6$. These figures are in good agreement with the physical behavior of nanofluids namely that the volume fraction of denser nanoparticles causes thinning of the momentum boundary layer. The rate of heat transfer is also reduced within the momentum boundary layer. The reason for this trend is that an increase in the volume of nanoparticles increases the overall thermal conductivity of nanofluids since the solid particles have higher thermal conductivity when compared to the base fluid.

The variation in δ and its effect on nanofluid velocity is shown in Figure 9 for $A = M = \phi = 0.2, \epsilon = 0.3$, $S = 0.4, \gamma = 0.6$. For the parametric value $\delta = 0.2, 0.6$ it

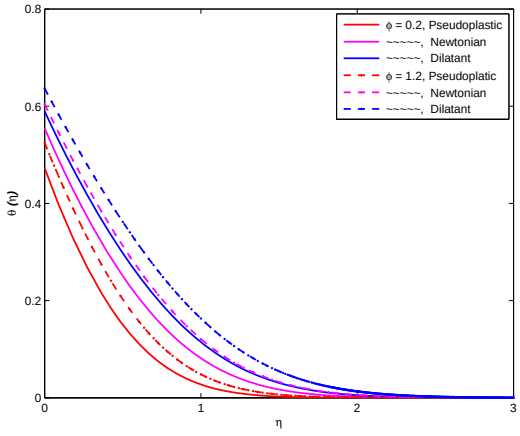

Figure 8: Influence of ϕ on temperature of a power-law nanofluid

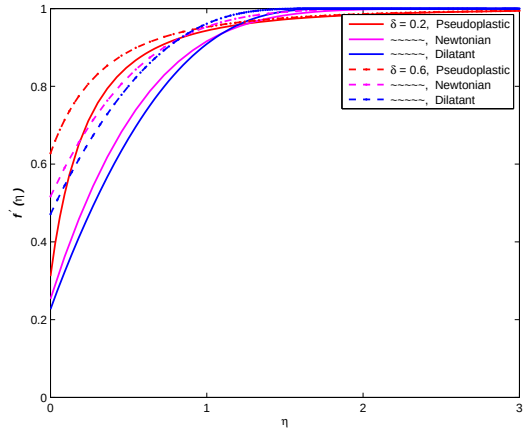

Figure 9: Influence of δ on velocity of a power-law nanofluid

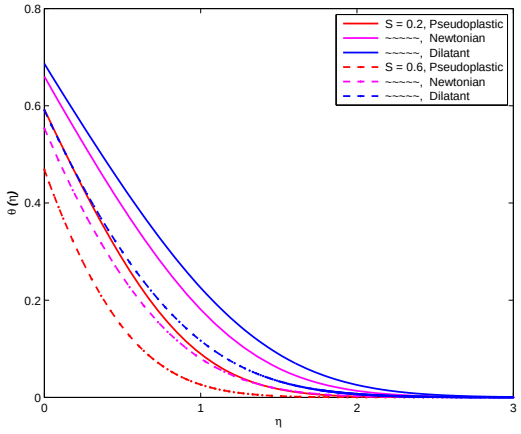

Figure 12: Influence of $S > 0$ on temperature of a power-law nanofluid

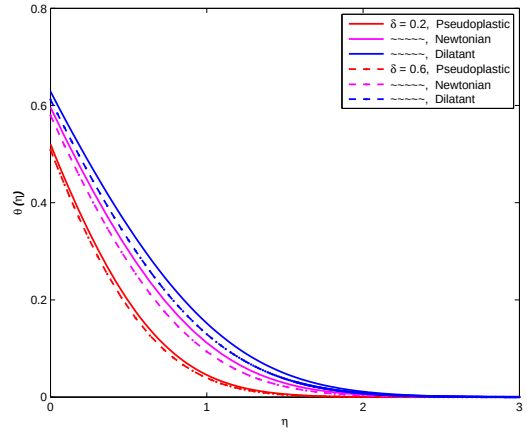

Figure 10: Influence of δ on temperature of a power-law nanofluid

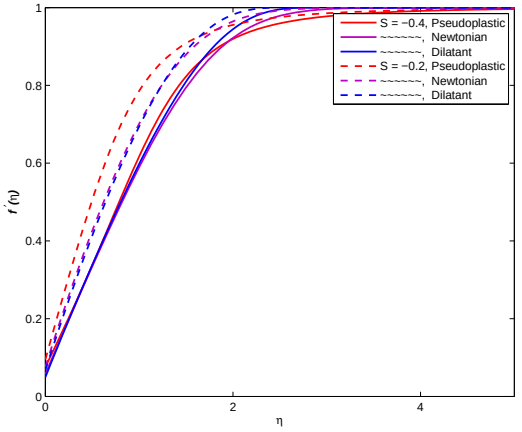

Figure 13: Effect of $S < 0$ on velocity of a power-law nanofluid

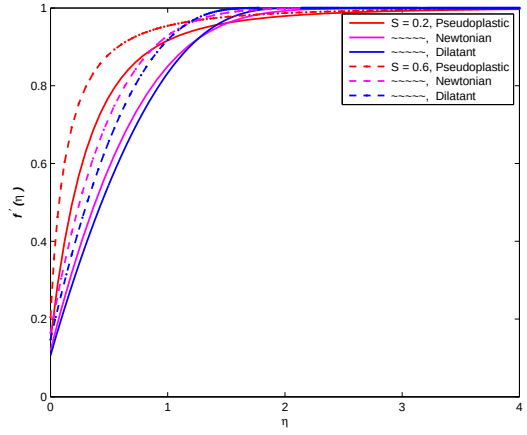

Figure 11: Influence of $S > 0$ on velocity of a power-law nanofluid

can be seen that the velocity for shear thinning, Newtonian and shear thickening fluids increases with increasing values of the velocity slip at the boundary. This expected behavior is due to positive values of nanofluid velocity at the boundary. As a result, thickness of the boundary layer will decrease when parameter δ increases. On the other hand, it is evident from Figure 10 that the surface slipperiness affects the temperature of the fluid inversely at the boundary, *i.e.*, an increase in slip parameter tends to decrease the temperature of the power-law nanofluid and enhance the rate of heat transfer.

The variation in S and its influence on motion and temperature of power-law nanofluids are shown in Figures 11-14, respectively. The momentum boundary layer thickness decreases with increasing values of $S > 0$ (suction parameter). This is because more fluid is transferred into the

Table 3: Nature of the skin friction coefficient and the Nusselt number with $a = 1.0$, $Pr = 6.2$

n	A	ϕ	ϵ	M	S	δ	γ	$-(f''(0))^n$	$-\theta'(0)$
0.4	0.1	0.20	0.3	0.6	0.2	0.1	0.1	1.4006	0.9700
1.0								1.0520	0.7444
1.4								0.8973	0.6679
1.4	0.1							0.8973	0.6679
	0.6							0.9150	0.6636
	1.6							0.9421	0.6568
1.4		0.05						0.7709	0.7966
		0.10						0.8121	0.7483
		0.15						0.8544	0.7059
		0.20						0.8975	0.6680
1.4			0.1					0.8975	0.7395
			0.3					0.8975	0.6680
			0.6					0.8975	0.5894
1.4				0.2				0.6917	0.6446
				0.6				0.8373	0.6540
				1.2				0.9591	0.6611
1.4					0.0			0.6511	0.5169
					0.2			0.8975	0.6680
					0.4			1.1502	0.8215
1.4						0.0		0.9484	0.6389
						0.2		0.8437	0.6913
						0.4		0.6542	0.7510
1.4							0.0	0.9022	0.7088
							0.2	0.8935	0.6311
							0.3	0.8899	0.5976

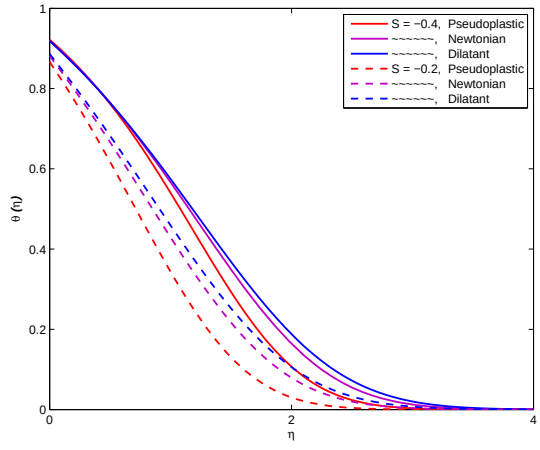

Figure 14: Effect of $S < 0$ on temperature of a power-law nanofluid

boundary layer through the porous surface. From Figure 13, it may be noted that the boundary layer thickness increases with increase in injection $S < 0$. The imposition of suction on the surface causes reduction in the thermal boundary layer thickness and injection causes an increase in the thermal boundary layer thickness.

Table 3 presents the nature of the skin friction coefficient of the wall (velocity gradient) and Nusselt number (temperature gradient) at the boundary for the MHD slip flow of a power-law nanofluid. Similarly the nature of the skin friction coefficient and Nusselt number is observed for pseudoplastic, newtonian and dilatant nanofluids. Similar nature is observed for pseudoplastic, newtonian and dilatant nanofluids. Therefore, numerical computations are only presented for $n = 1.4$ in Table 3. It can be seen that pseudoplastic fluids have the highest values and the dilatant fluids have the lowest values of the skin friction coefficient and Nusselt number. The lowest rate of effective viscosity for pseudoplastic fluids is the reason behind this. Moreover, it is evident that the velocity gradient at the boundary increases with increasing values of parameters A, ϕ, M, and S; whereas a reduction in the skin friction coefficient is observed for increasing values

of δ and γ. Increase in the velocity gradient at the boundary corresponds to thinning of the momentum boundary layer thickness and decrease in the velocity of the nanofluids. The decreasing trend shows that the fluid velocity is approaching the free stream velocity. It is observed from Table 3, that the Nusselt number increases with enhancement in the strength of applied transverse magnetic field M, δ the velocity slip coefficient of the surface and the S the suction/injection parameter. Increasing values of parameters A, ϕ, ϵ and γ decrease the Nusselt number.

The simplified model for flow and heat transfer analysis of a power-law nanofluid presents a qualitative analysis that can be quantified to calculate the thermal efficiency of the system. Results can be generalized to include the effects of variable viscosity, variable porosity and heat transfer of non-Newtonian nanofluids (see for example [36, 37]). Comparisons can be drawn between the results of the presented model and nano scale flow. Alternatively, the present model can be solved by employing semi-analytical methods [19, 36, 38].

5 Concluding remarks and future work

In this work the principal effects of variable viscosity, variable thermal conductivity and applied transverse magnetic field on slip flow and heat transfer characteristics of a power-law nanofluid over a porous flat surface have been analyzed numerically. To the best of the authors' knowledge no such study has previously been presented in the literature. The governing system of PDEs was transformed into a system of ODEs and then solved numerically. Numerical computations performed for temperature and velocity variation of Cu-water nanofluid within the boundary layer were presented through graphs and tables. Parametric effects of different governing parameters on velocity and temperature profiles were discussed. It is concluded that:

1. Pseudoplastic nanofluids have the highest skin friction coefficient and dilatant fluids have the lowest skin friction coefficient. The highest rate of heat transfer is observed for $n < 1$ and the lowest for the case $n > 1$
2. Increase in nanofluid viscosity and volume fraction of nanoparticles decreases the velocity and increases the temperature of nanofluids within the boundary layer. This will reduce the heat transfer rate and enhance thickness of the momentum boundary layer
3. Increase in strength of the applied transverse magnetic field and suction velocity increases the velocity and decreases the temperature distribution in the boundary layer
4. Increase in both velocity slip and thermal slip reduces thickness of the momentum boundary layer, whereas increase in slip velocity enhances and thermal slip reduces the rate of heat transfer.

References

[1] Choi S. U. S., Enhancing thermal conductivity of fluids with nanoparticle in developments and applications of non-Newtonian flows, ASME IMECE, NY, USA, 1995.
[2] Eastman J. A. , Choi S. U. S. , Li S. , Thompson L. J. and Lee S., Enhanced thermal conductivity through the development of nanofuids, J. Mater. Res., 1997, 457, 3-11.
[3] Wang X., Xu X., and Choi S. U. S., Thermal conductivity of nanoparticle fluid mixture, J. Thermophys. Heat Tr., 1999, 13, 474-480.
[4] Keblinski P., Phillpot S. R., Choi S. U. S. and Eastman J. A., Mechanisms of heat flow in suspensions of nano-sized particles (nanofluids),Int. J. Heat Mass Transf., 2002, 45, 855-863.
[5] Yiamsawasd T., Dalkilic A. S. and Wongwises S., Measurement of specifc heat of nanofuids, Curr. Nanosci., 2012, 10, 25-33.
[6] Buongiorno J., Convective transport in nanofluids, ASME J. Heat Transf., 2006, 128, 240-250.
[7] Keblinski P., Eastman J. A., and Cahill D. G., Nanofuids for thermal transport, Mater. Today, 2005, 8, 36-44.
[8] Wang X. Q., Arun S. and Mujumdar S., Heat transfer characteristics of nanofluids: a review, Int. J. Therm. Sci., 2007, 46, 1-19.
[9] Akbarinia A., Abdolzadeh M. and Laur R., Critical investigation of heat transfer enhancement using nanofuids in micro channels with slip and non-slip flow regimes, Appl. Therm. Eng., 2011, 31, no. 4, 556-565.
[10] Uddin M. J., Pop I. and Ismail A. I. M., Free convection boundary layer flow of a nanofuid from a convectively heated vertical plate with linear momentum slip boundary condition, Sains Malays., 2012, 4, 1175-78.
[11] Ibrahim B. and Shankar W., Mhd boundary layer flow and heat transfer of a nanofluid past a permeable stretching sheet with velocity, thermal and solutal slip boundary conditions., Comput. Fluids, 2013, 75, 1-10.
[12] Uddin W. A. N. and Khan M. J., g-jitter mixed convective slip flow of nanofluid past a permeable stretching sheet embedded in a darcian porous media with variable viscosity., PLoS ONE, 2014, 9, 9379-84.
[13] Nasrin R., and Alim M. A., Entropy generation by nanofluid with variable thermal conductivty and viscosity in a flate plate solar collector, Int. J. Eng. Sci Tech., 2015, 7, no. 2, 80-93.
[14] Yazdi M. E., Moradi A. and Dinarvand S., Mhd mixed convection stagnation- a stretching vertical plate in porous medium filled with a nanofluid in the presence radiation, Arab. J. Sci. Eng., 2014, 39, 2251-61.

[15] Ellahi R., Hassan M. and Zeeshan A., Study on magnetohydrodynamic nanofluid by means of single and multi-walled carbon nanotubes suspended in a salt water solution, IEEE Trans. Nanotechnol., 2015, 14, 726-34.
[16] Afzal K. and Aziz A., Transport and heat transfer of time dependent mhd slip flow of nanofluids in solar collectors with variable thermal conductivity and thermal radiation, Results in Physics, 2017. 6, 746-753.
[17] Abbasi M., Heat analysis in a nanofluid layer with fluctuating temperature,Iran. J. Sci. Technol. Trans. A Sci., 2017, 14, 1-11.
[18] Ali F., Sheikh N., Saqib M., and Khan A., Hidden phenomena of an mhd unsteady flow in porous medium with heat transfer, J. Nonlin. Sci. Lett. A., 2017, 8, 101-116.
[19] Vahabzadeh A., Fakour M., and Ganji D., Study of mhd nanofluid flow over a horizontal stretching plate by analytical methods, Int. J. PDE Appl., 2017, 2, No.6, 96-104.
[20] Beg A. O., Khan M., Karim I., Alam M., and Ferdows M., Explicit numerical study of unsteady hydromagnetic mixed convective nanofluid flow from an exponentially stretching sheet in porous media, Appl. Nanosci., 2014, 4, 943-957.
[21] Santra A., Sen S., and Chakraborty N., Study of heat transfer due to laminar flow of copper-water nanofluid through two isothermally heated parallel plates, Int. J. Therm. Sci., 2009, 48, 391-400.
[22] Ellahi R., Raza M., and Vafai K., Series solutions of non-newtonian nanofluids with Reynolds model and Vogela model by means of the homotopy analysis method, Math. Comput. Model., 2012, 55, 1876-91.
[23] Nadeem S., Rizwan Ul Haq and Khan Z. H., Numerical study of mhd boundary layer flow of a maxwell fluid past a stretching sheet in the presence of nanoparticles, J. Taiwan. Inst. Chem. Eng., 2014, 45, 121-26.
[24] Ramzan M. and Bilal M., Time dependent mhd nano-second grade fluid flow induced by permeable vertical sheet with mixed convection and thermal radiation, PLoS ONE, 2015, 10, 25.
[25] Hayat T., Hussain M., Shehzad S. A., and Alsaedi A., Flow of a power-law nanofluid past a verticle stretching sheet with a convective boundary condition, J. Appl. Mech. Tech. Phys., 2016, 57, 173-179.
[26] Khan M. and Khan W. A., Mhd boundary layer flow of a power-law nanofluid with new mass flux condition, AIP Advan., 2016, 6, 2119-26.
[27] Aziz T., Aziz A., and Khalique C., Exact solutions for stokes' flow of a non-newtonian nanofluid model: a lie similarity approach, Zeitschrift für Naturforschung A, 2016, 71, 621.
[28] Farooq U., Hayat T., Alsaedi A., and Liao S., Heat and mass transfer of two-layer flows of thirdgrade nano-fluids in a vertical channel, Appl. Math. Comput, 2016, 242, 528-540.
[29] Hussain S., Aziz A., Aziz T. and Khalique C. M., Slip flow and heat transfer of nanofluids over a porous plate embedded in a porous medium with temperature dependent viscosity and thermal conductivity, Appl. Sci., 2016, 6, 376.
[30] Shehzad S. A., Abdullah Z., Alsaedi A., Abbaasi F. M., and Hayat T., Boundary thermally radiative three-dimensional flow of jeffrey nanofluid with internal heat generation and magnetic field, J. Magn. Magn. Mater., 2016, 397, 108-114.
[31] Maxwell J., A Treatise on Electricity andMagnetism (Second edition), Clarendon Press, Oxford, UK, 1881.
[32] Bhaskar T. S. P, Poornima N. R., Influence of variable thermal conductivity on mhd boundary layer slip flow of ethylene-glycol based cu nanofluids over a stretching sheet with convective boundary condition., Int. J. Eng. Math., 2014, 9051-58.
[33] Arunachalam N. and Rajappa M., Forced convection in liquid metals with variable thermal conductivity and capacity, Acta Mech., 1978, 31, 25-31.
[34] Hirschhorn J., Madsen M., Mastroberardino A. and Siddique J. I., Magnetohydrodynamic boundary layer slip flow and heat transfer of power law fluid over a flat plate, J. Appl. Fluid Mech., 2016, 9, 11-17.
[35] Shankar B. and Yirga Y., Unsteady heat and mass transfer in mhd flow of nanofluids over stretching sheet with a non-uniform heat source/sink, World Academy of Science, Engineering and Technology Int. J. Math. Comput. Stat. Natural Phys. Eng., 2013, 7, 1766-1774.
[36] Gul T., Shayan W., Ali F., Khan I., Shafie S., and Sheikh N. A., Analysis of time dependent third grade fluid in wire coating, J. Nonlinear Sci. Letts. A, 2017, 8, 374-388.
[37] Mahmood A., Aziz A., Jamshed W. and Hussain S., Mathematical model for thermal solar collectors by using magnetohydrodynamic maxwell nanofluid with slip conditions, thermal radiation and variable thermal conductivity, Results in Physics, 2017, 7, 3425-3433.
[38] Hajmohammadi M., Nourazar S., and Manesh A., Semi-analytical treatments of conjugate heat transfer, J. Mech. Eng. Sci., 2012, 227, 492-503.